Pilocarpine-induced dilation of Schlemm's canal and prevention of lumen collapse at elevated intraocular pressures in living mice

Guorong Li[1,4], Sina Farsiu[1], Stephanie J. Chiu[4], Pedro Gonzalez[1], Elke Lütjen-Drecoll[2], Darryl R. Overby[3] and W. Daniel Stamer[1,4]

[1]Department of Ophthalmology, Duke University, Durham, NC

[2]Department of Anatomie II, University Erlangen-Nürnberg, Germany

[3]Department of Bioengineering, Imperial College London, London UK

[4]Department of Biomedical Engineering, Duke University, Durham, NC

Running Title: OCT imaging of SC in living mice

Key Words: aqueous humor, glaucoma, trabecular meshwork, optical coherence tomography, ocular hypertension, pilocarpine, speckle variance

Word Count: 4415

Abstract word count: 250

Corresponding Author:

W. Daniel Stamer
Duke University
DUMC 3802
Durham, NC 27710
919-684-3745
dstamer@eyes.arizona.edu

Abstract

Purpose: The goal was to assess effects of intraocular pressure (IOP) and pilocarpine-induced ciliary muscle contraction on conventional outflow pathway tissues in living anesthetized mice.

Methods: IOP was controlled by intracameral cannulation of mouse eyes while imaging using spectral domain optical coherence tomography (SD-OCT). Time-lapse sagittal SD-OCT sections through Schlemm's canal (SC) were acquired while changing IOP stepwise between 10 and 45 mmHg. After topical application of 1% pilocarpine, the series of IOP steps and imaging were repeated. Effects of pilocarpine on IOP and outflow facility in living mice were verified by rebound tonometry and flow measurements at 3 different IOPs, respectively. *In vivo* OCT images were compared to eyes analyzed by standard histology.

Results: In living mice imaged by SD-OCT, the lumen of SC progressively collapsed with increasing IOP, reaching near complete closure at 20 mmHg. SC collapse was reversible, with the lumen opening within minutes after returning IOP from 45 to 10 mmHg. Pilocarpine-induced ciliary muscle contraction changed SC lumen area by 131.6±21% compared to untreated controls at 10 mmHg, opened the trabecular meshwork and prevented complete collapse of the SC lumen at higher pressures. Similar results were observed by standard histology. Pilocarpine increased outflow facility 4-fold (p= 0.02) and lowered IOP (16.46 ± 2.23 versus 11.08 ± 2.28 mmHg, p = 0.03).

Conclusions: SD-OCT was effective at visualizing changes in SC lumen in living mice. Results with pilocarpine are consistent with the concept that a primary role for the ciliary muscle is to prevent collapse of SC.

Introduction

Clinically, non-selective muscarinic receptor agonists such as pilocarpine are used to rapidly lower intraocular pressure (IOP) by increasing conventional outflow facility[1-3]. Pilocarpine increases conventional outflow by binding to and activating muscarinic M_3 receptors on ciliary smooth muscle cells, stimulating contraction[4]. The ciliary muscle in primates is compound, having circular and longitudinal fibers. Anchored to the choroid, longitudinal ciliary muscle contraction pulls on tendons that extend into the conventional outflow tract, terminating in the trabecular meshwork and inner wall of Schlemm's canal (SC)[5, 6]. Functional consequences of ciliary muscle contraction appear to include expansion of the juxtacanalicular portion of the trabecular meshwork and opening of the lumen of SC. Ciliary muscle tone is critical for proper functioning of the conventional outflow tract because at elevated IOP the lumen of SC is prone to collapse[7, 8]. Hence, in addition to the presence of septae (struts) that span from the inner to outer wall to prop the SC lumen open near collector channels, tension from the ciliary muscle helps keep open SC in between collector channels; maintaining flow of aqueous humor into the canal and return to the systemic circulation.

In addition to outflow effects, pilocarpine-stimulated ciliary muscle contraction in primates results in the inward and anterior movement of the circular ciliary muscle fibers[9]. Displacement of ciliary muscle mass releases tension on the zonules of the crystalline lens, thereby enabling accommodation as the lens rounds up. In parallel, pilocarpine interacts with muscarinic receptors in the iris sphincter muscle cells to constrict the pupil. Due to availability of drugs without these two later effects (accommodation and miosis), pilocarpine is not generally used as a first line treatment of ocular hypertension. However, due to its rapid, efficacious and transient effects, pilocarpine is often used for a variety of ocular applications including the acute treatment of ocular hypertension in clinical emergencies.

Interestingly, mice do not accommodate, but have a ciliary muscle; suggesting that a primary purpose of the ciliary muscle in mice (and possibly humans) is for the regulation of outflow facility[10]. Similar to human, mouse eyes have two layers of longitudinal ciliary muscle fibers that converge onto "tips", which pull on tendons that extend into the trabecular meshwork and inner wall of SC[10]. Unlike other non-accommodating species like porcine and bovine, mice have a conventional outflow tract that is anatomically, physiologically and pharmacologically very similar to human[11, 12]. While some anatomical features are not identical between human and mice (discontinuous scleral spur and anterior versus posterior fixation of TM), treatment of mouse eyes with pilocarpine lowers IOP[13, 14], and perfusion of enucleated mouse eyes with

pilocarpine results in increased outflow facility[10]; consistent with its role in modulating conventional outflow function like human. Effects of pilocarpine in mouse and primate eyes is in contrast to pilocarpine effects in bovine eyes, which does the opposite and decreases outflow facility[15, 16]. Taken together, these data are consistent with anatomical and pharmacological differences between eyes with angular aqueous plexus, like bovine or porcine, and eyes with SC, like rodents and primates.

While the effects of pilocarpine on ciliary muscle contraction and lens rounding have been documented in living monkeys by optical coherence tomography (OCT)[9], effects of pilocarpine on conventional outflow tissues were not resolved. Due to their relatively thin sclera and large SC lumen, the conventional outflow pathway of mice is a good candidate for *in vivo* microscopic imaging. Several recent studies have address the problem of imaging SC in human eyes[17-20], However, documentation of SC behavior of mice with OCT has different technical obstacles than human (i.e. small eye, blood in canal, and need for iridotomy to prevent anterior chamber deepening). Recent improvements in the resolution of commercial OCT systems, customized for murine eye imaging, now enable direct visualization of conventional outflow behavior in living mice. Using a custom built mouse housing platform for a commercial spectral domain (SD) OCT system, the goal of the present study was twofold: (i) to explore and optimize techniques to image the conventional outflow pathway of mice *in vivo* using SD-OCT and (ii) to examine the effects of elevated IOP on SC lumen collapse in the presence and absence of pilocarpine in living mice. To be complete, we also examined the effects of pilocarpine on intraocular pressure and conventional outflow facility in living mice.

Methods

Animals

Mice were handled in accordance with animal care and use guidelines of Duke University and in compliance with the ARVO Statement for the Use of Animals in Ophthalmic and Vision Research. CD1 mice were purchased from the Jackson Laboratory (Bar Harbor, Maine, USA), bred/housed in clear cages and kept in rooms at 21°C with a 12 h: 12 h light-dark cycle. Mice were used at ages between 4 to 8 weeks old. Due to the potential effect of posterior iris bowing and anterior chamber deepening[21], we performed iridotomies to equalize pressure on both sides of iris. Iridotomy was conducted on the left eye of all mice one to two weeks before OCT imaging: Briefly, mice were anesthetized by intraperitoneal injection of Ketamine (100mg/kg) and Xylazine (10mg/kg). A drop of Proparacaine, a topical anesthetic, was applied to the left eye. A clear-corneal wound was made with a Beaver 75 blade under an operating microscope. A 0.12 forceps was used to grasp the iris and a small iridotomy hole (~2 mm) was cut using Vannes scissors. Erythromycin, a topical antibiotic ointment was applied to the cornea, and the animals were maintained on a warm water-circulating blanket until recovery from the anesthesia.

OCT Imaging

In vivo imaging was performed utilizing an Envisu R2200 Ultra-high-resolution SD-OCT system (Bioptigen Inc., Research Triangle Park, NC). This 840 nm SD-OCT system utilized customized 180 nm Superlum Broadlighter source providing two micron axial resolution, and a 12mm telecentric lens bore for anterior segment OCT imaging.

For OCT experiments, mice were anesthetized as described for iridotomy, then placed on a custom-made OCT imaging mount that we designed and manufactured specifically for imaging mice (Figure 1). This imaging mount was equipped with an onboard micromanipulator to insert a glass cannula into the temporal quadrant of the anterior chamber to control and measure IOP. Moreover, the imaging mount fit perfectly into the Bioptigen OCT alignment stage to accurately position and hold the OCT probe for imaging sessions.

A pulled glass micro-needle was filled with phosphate buffered saline (PBS) and inserted into the mouse anterior chamber. The micro-needle was connected to both a manometric column to adjust IOP and a pressure transducer to continuously monitor IOP levels (using PowerLab software). The OCT probe was aimed at the inferior lateral limbus and the image was centered and focused at SC. While collecting images at the same region of SC, the mouse eye was subjected to a series of IOP steps (10, 12, 15, 17, 20, 22, 25, 35, 45 and back to 10 mmHg) by

adjusting the height of fluid reservoir. At each IOP step, a sequence of 100 repeated OCT B-scans (each with 1000 A-scans spanning 1 mm in lateral length) from spatially very close positions was captured. Image registration and SC lumen area analyses were performed utilizing ImageJ (freeware; National Institutes of Health, Bethesda, MA) StackReg registration plug-in[22]. Each averaged OCT image was opened into ImageJ software (freeware; National Institutes of Health, Bethesda, MA) and SC area was marked and area calculated. Estimates of lumen borders were verified with the lumen edges observed in live video; comparing stationary lumen edges with moving reflectors (blood cells in lumen). Area calculations at each pressure level were normalized to untreated 10 mmHg control group. All images were analyzed on two separate occasions (over two months apart) by the same trained observer (GL) to assess intra-observer variability. Intra-observer reliability was calculated by comparing the average difference between normalized SC lumen area measurements at the two sessions (over the entire range of IOPs)

For pilocarpine experiments, untreated eyes were imaged sequentially at each pressure step, and then the IOP was set back to 10 mmHg for 10 min. A drop of 1% pilocarpine was then given to the mouse eye, and kept for another 10 min. The eyes were then subjected to the same pressure sequence as before, and images were captured at each pressure level.

OCT Image Post-Processing

High signal-to-noise-ratio images of the anterior segment were generated at each IOP step by registering and averaging each sequence of repeated OCT B-scans. Rigid body image registration was performed using the ImageJ (freeware; National Institutes of Health, Bethesda, MA) StackReg registration plug-in[18].

To visualize regions with fluid flow (e.g. blood vessels and SC), we generated speckle variance images[23-25] as a complementary source of information to the averaged image. Since speckle patterns on an image change with time as a result of motion, high variances across images in time are expected in regions with fluid flow, whereas low variances corresponding to the detector noise are expected for static tissue. Accordingly, we computed the intensity variance across three consecutive repeated and registered B-scans (e.g. for scans 1-3, scans 2-4, etc.), and the mean across the 98 variance images resulted in the final speckle variance image.

Due to the high-resolution imaging capabilities of our OCT system and the prone position of the animals, which roughly aligned the eye and heart along the same horizontal plane, we were able to visualize red cells inside the SC lumen as a result of venous congestion. While the

presence of red cells facilitated visualization of the SC lumen (and surrounding vessels), it also introduced some blurring to the averaged images. These artifacts were reduced by locally enhancing the image using adaptive histogram equalization[26], where the regions of interest were isolated through thresholding of the speckle variance image.

Histology

Mice with iridotomized eyes were anesthetized systemically by intraperitoneal injection of Ketamine (100mg/kg) and Xylazine (10mg/kg) and then 10 µl of 1% pilocarpine eye drop was applied to one eye. Twenty minutes later, two glass micro-needles connected to a fluid reservoir filled with fixative solution (2.5% paraformaldehyde, 0.75% glutaraldehyde) were inserted into anterior chamber of each eye. Both eyes were perfused simultaneously at IOPs 10, 25, or 45 mmHg for 1h. After perfusion, mice were euthanized and the eyes were collected and immersed into fixative solution overnight at 4˚C. The eyes were bisected, posterior segments and lens were removed. The anterior segments were cut into four quadrants and each quadrant was embedded into Epon. Blocks were cut into 0.5 µm semi-thin sections and stained with 1% methylene Blue. The images were captured digitally using light microscopy.

Outflow facility

Outflow facility measurements were conducted in living mouse eyes as previously described[27]. Briefly, for bilateral measurements two micropipette manipulators were used to place a microneedle in each mouse eye. Each microneedle was connected to a pressure tubing (0.05 inch inner diameter (Mallinckrodt, Hazelwood, Missouri, USA) leading to a three-way stopcock. The stopcock was connected to a 5-mL syringe filled with PBS and to pressure tubing connected to a second three-way stopcock. A pressure transducer (Honeywell model 142PC05D, Honeywell Sensing and Control, MN, USA) and a vertical column of fluid (RenaPulse™ Tubing 0.08 mm ID, Braintree Scientific Inc. Braintree, MA, USA) were connected to the second stopcock. The transducer was connected to a PowerLab data acquisition system (ML870/P PowerLab 8/30, ADInstruments, Colorado Springs, Colorado, USA) linked to a computer running PowerLab software. One glass column (0.05 mm ID, Sulter Instrument Co., Novato, CA) was connected to the top of the vertical pressure tubing to ensure that the liquid was vertical and the inner diameter was uniform for outflow calculations. The height of the fluid in the column was adjusted using a fluid-filled syringe. Transducers were calibrated prior to each experiment to ensure accurate pressure measurements. The height of fluid of the column set the pressure in the system. The fluid exiting the system was proportional to the decline in height of the column over time, and thereby was used to determine the flow

rate based on the dimensions of the fluid column. The average pressure over 10 minutes was used due to slight decline in pressure over time. Outflow facility data were excluded if the mouse died or leaking occurred during outflow facility measurements. Flow was measured at three different pressures (~17, 24 and 34 mmHg), a linear regression analysis was performed and slopes of pressure-flow relationships were compared between control and pilocarpine (topically treated) eyes to determine outflow facility.

Intraocular Pressure

IOP was measured in iridotomized eyes following 1% pilocarpine treatment in living mouse eyes using rebound tonometry (TonoLab). Briefly, mice were lightly anesthetized with Ketamine (50mg/kg) and Xylazine (5mg/kg) to limit IOP effects and watched for time when they just stopped moving (light sleep). IOP was immediately measured. Each IOP level was the average of six measurements from the same eye. After collection of IOPs from untreated eyes, 10 µl of 1% pilocarpine eye drop was given and IOP was measured at 20, 40, 120 and 210 min after treatment. Liquid around the eyes was removed using a Kimwipe before each series of IOP measurements. All mice were lightly anesthetized during IOP measurements, except at the 210 min time point when mice were just awakening from anesthesia.

Statistical analysis

Statistical significance between groups was assessed by either the Mann–Whitney *U*-test for comparing data from different eyes or paired student *t*-tests for comparing data from same mouse eyes. A value of $p<0.05$ was considered statistically significant.

Results

The OCT probe was pointed toward the inferior lateral limbus region of mouse eyes *in vivo*, focusing on the iridio-corneo angle at an open SC lumen, appearing similar to observed previously by standard histology (Supplemental Figure 1). A comparison of the three types of OCT images that are provided in figure 2 to view behavior of SC, averaged intensity, contrast enhanced and speckle variance. Inside blood vessel lumens, including SC we saw "speckling", presumably caused by red cells during live imaging. Speckling caused some blurring in SC or vessels in processed images after averaging, but made SC lumen walls easily identifiable as seen using information from both enhanced and speckle variance images. In speckle variance images, speckling features from above cast a shadow on structures below, making lower boundaries ambiguous.

Behavior of SC in response to IOP

Once imaging techniques with mice were optimized, we then monitored SC and TM behavior in response to elevated IOPs *in vivo*. The sequence of left hand images in figure 3 reveals the behavior of the conventional outflow pathway as evidenced by decrease in SC lumen area with each pressure step. While untouched images are shown in figure 3, contrast enhanced images are also provided to highlight SC lumen at each pressure step (Supplemental Figure 2). Although we were unable to detect changes in the TM, at 20 mmHg the SC canal lumen is almost entirely collapsed. However, we often observed the distal ends of the canal partially open. Moreover, we noticed that SC in these young mice fully collapses around 35 mmHg, but readily reopens to their initial dimensions upon returning IOP to 10 mmHg. Shown in figure 4 is combined analysis of SC lumen area taken from different mice exposed to sequential pressure gradients and normalized to initial dimensions at 10 mmHg. To quantify area of SC, lumen was marked (as in Figure 2) and the area was calculated on averaged intensity images using ImageJ. Edges of lumen for each condition were verified using live video of experiment, comparing stationary lumen edges with moving reflectors in lumen. Intra-observer variability was low and reliability of measurements was high, having only a 13.8±11.5% difference in two measurements of each image on two separate occasions by a single trained observer (GL).

Effects of pilocarpine on mouse outflow pathway

Using pilocarpine, we tested the idea that ciliary muscle contraction opposes SC collapse experimentally in living mice. Using the same mouse eyes that were subjected to the first set of pressure steps without treatment; we retested response of SC after the application of 1%

pilocarpine. Upper right panel in figure 3 shows that pilocarpine rapidly widened SC (within 10 min) in eyes held at the 10 mmHg level by 131.6±21% compared to pre-treatment levels. Concomitantly, the anterior lamellated trabecular meshwork was pulled inward and expanded into an open fan-like shape that widened approaching the anterior chamber (arrows in figure 3). In contrast, the angle between the cornea and iris (36.9^{o}±3.5 versus 37.8^{o}±2.6) and dimensions of various scleral vessels (marked by hash marks in figure 3) remained unchanged. Pilocarpine-treated eyes were then subjected to sequential pressure steps as before (right hand panels of figure 3). At every pressure tested, the lumen area was significantly wider (except at 35 mmHg) in the presence of pilocarpine. Importantly, at 20 mmHg where the SC lumen in controls was almost completely collapsed, the SC lumen in eyes treated with pilocarpine was still about 50% of the original area. Moreover, even at the highest pressure step (45 mmHg), portions of SC were still open. When IOP was dropped back to 10 mmHg, SC canal dimension returned to near baseline levels. Combined data derived from images of 4-5 mice treated with pilocarpine are compared to untreated animals in figure 4. Confirmation of pilocarpine actions on intraocular tissues in treated mice is clearly visible by closing of the pupil (usually within 5 minutes), and also by OCT (Supplemental Figure 3); where the iris sphincter muscle is contracted resulting in thinning of iris near iridio-corneo angle.

Speckle Variance Analysis of Blood Vessels in Angle

Figure 5 shows speckle variance OCT equivalents of the averaged images of iridio-corneo angle tissues containing SC lumen in figure 3. The intensity of the speckling pattern corresponding to the flow in the regions associated with SC and downstream scleral vessels decreases as IOP increases (left panels). In contrast, the speckling pattern corresponding to the flow in the regions associated with neighboring scleral vessels remain relatively unchanged at different IOPs (except slight changes associated with the slight motion caused by the mouse breathing pattern). In pilocarpine treated eyes speckling in SC decreases with increasing IOP, but is visible at all pressure steps, consistent with an open lumen.

SC lumen area in response to IOP gradients and pilocarpine using standard histology

Similar to results obtained in living mice with OCT, histology results in figure 6 show that SC lumen area in pilocarpine-treated eyes was larger than control, whether fixed by immersion at spontaneous IOP or perfusion fixation at 10 mmHg. Moreover, we observed that SC lumen was larger in pilocarpine-treated eyes at each of three pressure steps tested (10, 25 and 45 mmHg). Pilocarpine appeared to prevent complete SC collapse that was observed at 45 mmHg in untreated control eyes. Fixation seemed not to alter to the lumen of Schlemm's canal. However,

the appearance of the trabecular meshwork depended upon fixation conditions, and presumably on the location of the lens and iris that cannot be reliably kept in place during histological sectioning.

Pilocarpine effects on outflow facility and IOP in living mice

To relate changes in SC lumen area observed by OCT with traditional functional measures, we examined effects of pilocarpine on conventional outflow facility and IOP in two cohorts of living mice. Figure 7 shows the pressure-flow relationship of paired mouse eyes, one treated topically with PBS and the contralateral eye treated topically with 1% pilocarpine. The anterior chamber of eyes were cannulated and subjected to three pressure steps (17, 24 and 34 mmHg) and flow was measured at each pressure. Data show that flow was incrementally greater at 24 and 34 mmHg compared to control. Linear regression analysis of data in figure 7A show that outflow facility in pilocarpine-treated eyes was significantly different than controls, increasing by about 4-fold (figure 7B, p= 0.021). Interestingly, the Y-intercept (estimated flow at zero pressure) of control versus pilocarpine treatment in panel A is significantly different (0.1119±0.026 versus -0.1653±0.08 μl/min, p=0.02). Consistent with the outflow facility increase, we observed in panel C that IOP was less in pilocarpine-treated eyes compared to controls. Using rebound tonometry, we observed that IOP in pilocarpine-treated eyes was statistically lower 20 min after treatment (16.46 ± 2.23 versus 11.08 ± 2.28 mmHg, p = 0.027), reaching maximum effects at 40 minutes after treatment (9.17 ± 1.91 mmHg, p = 0.029). IOP began to return to normal levels at 120 minutes, reaching baseline levels by 210 minutes. By comparison, we were able to detect changes in outflow by 20 minutes, which were maintained for the duration of the experiment (~90 minutes).

Discussion

The present study for the first time documents drug and pressure-dependent responses of the conventional outflow pathway in a living animal. Data show that graded steps of IOP collapse SC in a step wise fashion, with the lumen almost completely collapsed at 20 mmHg. In contrast, at baseline IOP pilocarpine treatment of mouse eyes increases SC lumen area, widens the TM and prevents total collapse of SC lumen, even up to IOPs of 45 mmHg. Taken together, data demonstrate the value of OCT imaging of living mice and support a primary role for the ciliary muscle to pull on conventional outflow tissues and prevent SC collapse. Figure 8 summarizes the observed morphological changes in the mouse conventional outflow pathway in response to pilocarpine.

The pressure-dependent behavior of the conventional outflow tissues in response to changing IOPs was first proposed by Johnstone and Grant upon visualization of a dramatic outward expansion and reconfiguration of human and monkey outflow tissues after perfusion fixation at elevated IOPs[28]. In response to increasing pressure, they observed in histological samples that the spaces between trabecular meshwork beams and plates opened outward, the inner wall of SC was filled with giant vacuoles, ballooning and partially collapsing its lumen. Using a similar range of IOP challenges, we saw comparable inward to outward movement of mouse conventional outflow tissues by SD-OCT. Unfortunately, the SD-OCT device (with ~2 μm axial resolution) that we used does not have the resolution to visualize giant vacuoles at elevated IOPs. However, a newer generation of commercial SD-OCT machines are becoming available that have <1 μm axial resolution, which may be enough to visualize giant vacuole formation in living animals for the first time.

Complete collapse of human SC was observed at IOPs as low as 30 mmHg[28], compared to 20 mmHg in our experiments. Differences in the IOP required to fully collapse SC between humans and mice in these studies may be attributable to differences in the ciliary muscle tone or anatomical differences, such as the relative absence a scleral spur, that predisposes SC to collapse a lower IOPs in mice. Moreover, because the majority of past studies relied on histology, it was not possible for previous investigators to examine the reversibility of SC collapse within individual eyes. In contrast, because we were imaging living animals non-invasively, we were able to look at multiple pressure steps in a single animal and revert back to initial pressure and examine recovery in real time. The rapid recovery of SC lumen dimensions (within minutes) emphasizes the importance of the elastic network in the conventional tract in

mice and humans[10, 29]. It would be interesting in the future to see if there are differences in recovery from IOP challenges in young versus old mice.

As with previous studies, standard histology provided a good representation of snapshots of conventional outflow behavior at a specific IOP in the presence or absence of pilocarpine. Compared with OCT images, the general appearance of the SC lumen was dimensionally similar; however eyes were perfusion-fixed at a single IOP, so we could not obviously follow changes in SC lumen or flow within the SC lumen (speckle variance) over a range a pressures. It was interesting that we did not see a marked difference in appearance of SC lumen between perfusion and immersion fixed eyes treated with pilocarpine, suggesting that ciliary muscle contraction maintains SC dimensions during fixation. However, it was difficult to measure changes in the width of the trabecular meshwork in response to pilocarpine in histological sections on account of the lens and iris that are difficult to keep in place.

The mouse eye continues to prove a valuable model for studying human conventional outflow. Even though it does not accommodate, the mouse (like human) has a ciliary muscle that is connected via tendons to an elastic network in the trabecular meshwork that extends onto the inner wall of SC. Like previous studies in living mice[14], we observed a 3-7 mmHg drop in IOP following pilocarpine treatment. Effects are likely due to decreased inflow[30] and increased in outflow. The role of the ciliary muscle to modify conventional outflow function in mice was tested *in situ*, and contraction resulted in a doubling of outflow[10]. In the present study, we extended these finding to living mice, and found that ciliary muscle contraction increased conventional outflow 4-fold. The disparity in these magnitudes are unclear, but are likely due to differences in techniques used to measure facility and/or uncontrolled variables in living animal (i.e.: autonomic tone, blood supply, etc.). Regardless, the important point is that pilocarpine increases outflow, like human, and emphasizes the usefulness of mouse to study conventional outflow function. By OCT imaging, the increase in outflow facility in living mice appears to be caused by an expansion of SC lumen and widening of the TM, likely due to traction from the ciliary muscle contraction. Importantly, pilocarpine prevented SC collapse at susceptible IOPs. Thus, it appears that a primary role of the ciliary muscle is to keep open the conventional outflow tract and prevent SC collapse.

The source of the “speckling” in SC and neighboring blood vessels is unknown, but is likely caused by the presence of red blood cells. Appearance of images captured from vessels in the anterior eye angle of mice are similar to hundreds of OCT images published from other vascularized tissues containing the prominent OCT reflector, red cells. OCT images of mouse

SC are consistent with light and electron microscopic findings of red cells in SC of eyes that were freshly enucleated after an imaging session, fixed and processed (supplemental figure 4). Red cells appear in SC when venous pressure equals or exceeds intraocular pressure, as in the case when mice are imaged in the prone position. The character of speckling in SC and other neighboring vessels (both venous and arterial) is in contrast to the anterior chamber which appears black, without presence of obvious OCT reflectors.

Linear regression analyses of pressure-flow curves during outflow facility measurements show that pilocarpine significantly decreases the Y-intercept compared to control. Because significant changes in the Y-intercept have been interpreted as differences in pressure-independent outflow, it is tempting to speculate that pilocarpine may decrease uveoscleral flow in mouse eyes, as previously observed in primates whereby uveoscleral outflow of aqueous humor is shut down upon ciliary muscle contraction with pilocarpine[31]. These data provide additional evidence for functional similarities between human and mice in terms of aqueous humor dynamics.

With improved resolution and custom built mouse mounting stages (e.g. Figure 1), OCT technology now represents a valuable tool for learning about the normal physiology, pharmacology and pathology of the conventional outflow tract [17, 18, 19]. For example, questions about alterations in outflow tissue behavior with age, or with disease in recently established disease models in rodents for ocular hypertension[32-35] can now be specifically addressed. Since glaucoma is a group of diseases many of which impact conventional outflow function, it will be interesting to see if OCT can discriminate between these models with different genetic etiologies. Moreover, as new classes of drugs that target the conventional outflow pathway move through the drug company pipeline and are soon used by patients, the need to monitor drug efficacy becomes a reality. The present study clearly showed that effects of a currently prescribed drug, pilocarpine, on conventional outflow tissue behavior can be resolved by OCT. It will be interesting to see if effects of outflow drugs in development such as rho kinase inhibitors [36], adenosine A1 agonists [37] or nitric oxide donors [38, 39] can also be resolved. *Do these different classes of compounds impact conventional outflow differently? Can they be used as provocative tests to subtype glaucoma? Can treatment be "personalized" based upon responses?* Even though OCT has been successful at visualization of conventional outflow snapshots and identifying a narrowing of SC lumen in human glaucoma patients compared to age-matched controls[20], technological obstacles currently exist to prevent clinical utility of SD-OCT. The present study demonstrates the power of SD-OCT imaging of conventional outflow behavior in mice, where many issues can be worked out for future use in human.

Acknowledgements

The authors thank Prof. Pratap Challa for teaching us the iridotomy technique for mice and Ying Hao for help with histology studies, Jörg Pekarsky for preparing the schematic drawing, Prof. Joseph A. Izatt and Prof. Anthony N. Kuo for enlightening discussions during the course of this project. This work was supported in part by an NIH grants EY022359 and EY005722, North Carolina Biotechnology Center (IDG 2012-1015) and Research to Prevent Blindness Foundation.

References

1. Flocks M, Zweng HC. Studies on the mode of action of pilocarpine on aqueous outflow. *Am J Ophthalmol* 1957;44:380-386; discussion 387-388.

2. Barany EH. The mode of action of pilocarpine on outflow resistance in the eye of a primate (Cercopithecus ethiops). *Invest Ophthalmol* 1962;1:712-727.

3. Lutjen-Drecoll E. Structural factors influencing outflow facility and its changeability under drugs. A study in Macaca arctoides. *Invest Ophthalmol* 1973;12:280-294.

4. Gil DW, Krauss HA, Bogardus AM, WoldeMussie E. Muscarinic receptor subtypes in human iris-ciliary body measured by immunoprecipitation. *Invest Ophthalmol Vis Sci* 1997;38:1434-1442.

5. Rohen JW, Lutjen E, Barany E. The relation between the ciliary muscle and the trabecular meshwork and its importance for the effect of miotics on aqueous outflow resistance. A study in two contrasting monkey species, Macaca irus and Cercopithecus aethiops. *Albrecht Von Graefes Arch Klin Exp Ophthalmol* 1967;172:23-47.

6. Lutjen-Drecoll E, Wiendl H, Kaufman PL. Acute and chronic structural effects of pilocarpine on monkey outflow tissues. *Trans Am Ophthalmol Soc* 1998;96:171-191; discussion 192-175.

7. Hashimoto JM, Epstein DL. Influence of intraocular pressure on aqueous outflow facility in enucleated eyes of different mammals. *Invest Ophthalmol Vis Sci* 1980;19:1483-1489.

8. Moses RA, Arnzen RJ. The trabecular mesh: a mathematical analysis. *Invest Ophthalmol Vis Sci* 1980;19:1490-1497.

9. Glasser A, Croft MA, Brumback L, Kaufman PL. Ultrasound biomicroscopy of the aging rhesus monkey ciliary region. *Optom Vis Sci* 2001;78:417-424.

10. Overby DR, Bertrand J, Schicht M, Paulsen F, Lütjen-Drecoll E. The Three-Dimensional Structure of the Mouse Trabecular Meshwork, its Connections to the Ciliary Muscle and the Effect of Pilocarpine on Outflow Facility. *In review* 2013.

11. Lei Y, Overby DR, Boussommier-Calleja A, Stamer WD, Ethier CR. Outflow physiology of the mouse eye: pressure dependence and washout. *Invest Ophthalmol Vis Sci* 2010;52:1865-1871.

12. Boussommier-Calleja A, Bertrand J, Woodward DF, Ethier CR, Stamer WD, Overby DR. Pharmacologic manipulation of conventional outflow facility in ex vivo mouse eyes. *Invest Ophthalmol Vis Sci* 2012;53:5838-5845.

13. Avila MY, Carre DA, Stone RA, Civan MM. Reliable measurement of mouse intraocular pressure by a servo-null micropipette system. *Invest Ophthalmol Vis Sci* 2001;42:1841-1846.

14. Akaishi T, Odani-Kawabata N, Ishida N, Nakamura M. Ocular hypotensive effects of anti-glaucoma agents in mice. *J Ocul Pharmacol Ther* 2009;25:401-408.

15. Wiederholt M, Bielka S, Schweig F, Lutjen-Drecoll E, Lepple-Wienhues A. Regulation of outflow rate and resistance in the perfused anterior segment of the bovine eye. *Exp Eye Res* 1995;61:223-234.

16. Hubbard WC, Kee C, Kaufman PL. Aceclidine effects on outflow facility after ciliary muscle disinsertion. *Ophthalmologica* 1996;210:303-307.

17. Kagemann L, Wollstein G, Ishikawa H, et al. Identification and assessment of Schlemm's canal by spectral-domain optical coherence tomography. *Invest Ophthalmol Vis Sci* 2010;51:4054-4059.

18. Leung CK, Weinreb RN. Anterior chamber angle imaging with optical coherence tomography. *Eye (Lond)* 2011;25:261-267.

19. Usui T, Tomidokoro A, Mishima K, et al. Identification of Schlemm's canal and its surrounding tissues by anterior segment fourier domain optical coherence tomography. *Invest Ophthalmol Vis Sci* 2011;52:6934-6939.

20. Kagemann L, Wollstein G, Ishikawa H, et al. Visualization of the conventional outflow pathway in the living human eye. *Ophthalmology* 2012;119:1563-1568.

21. Brubaker RF. The effect of intraocular pressure on conventional outflow resistance in the enucleated human eye. *Invest Ophthalmol* 1975;14:286-292.

22. Thevenaz P, Ruttimann UE, Unser M. A pyramid approach to subpixel registration based on intensity. *IEEE Trans Image Process* 1998;7:27-41.

23. Mariampillai A, Standish BA, Moriyama EH, et al. Speckle variance detection of microvasculature using swept-source optical coherence tomography. *Opt Lett* 2008;33:1530-1532.

24. Kim DY, Fingler J, Werner JS, Schwartz DM, Fraser SE, Zawadzki RJ. In vivo volumetric imaging of human retinal circulation with phase-variance optical coherence tomography. *Biomed Opt Express* 2011;2:1504-1513.

25. Hendargo HC, Estrada R, Chiu SJ, Tomasi C, Farsiu S, Izatt JA. Automated non-rigid registration and mosaicing for robust imaging of distinct retinal capillary beds using speckle variance optical coherence tomography. *Biomed Opt Express* 2013;4:803-821.

26. Zuiderveld K. Contrast Limited Adaptive Histograph Equalization. *Graphic Gems IV San Diego: Academic Press Professional* 1994;474-485.

27. Li G, Gonzalez P, Camras LJ, et al. Optimizing gene transfer to conventional outflow cells in living mouse eyes. *Exp Eye Res* 2013;109:8-16.

28. Johnstone MA, Grant WG. Pressure-dependent changes in structures of the aqueous outflow system of human and monkey eyes. *Am J Ophthalmol* 1973;75:365-383.

29. Rohen JW, Futa R, Lutjen-Drecoll E. The fine structure of the cribriform meshwork in normal and glaucomatous eyes as seen in tangential sections. *Invest Ophthalmol Vis Sci* 1981;21:574-585.

30. Nagataki S, Brubaker RF. Effect of pilocarpine on aqueous humor formation in human beings. *Arch Ophthalmol* 1982;100:818-821.

31. Crawford K, Kaufman PL. Pilocarpine antagonizes prostaglandin F2 alpha-induced ocular hypotension in monkeys. Evidence for enhancement of Uveoscleral outflow by prostaglandin F2 alpha. *Arch Ophthalmol* 1987;105:1112-1116.

32. Zode GS, Kuehn MH, Nishimura DY, et al. Reduction of ER stress via a chemical chaperone prevents disease phenotypes in a mouse model of primary open angle glaucoma. *J Clin Invest* 2011;121:3542-3553.

33. Sheppard J, Hayes S, Boote C, Votruba M, Meek KM. Changes in corneal collagen architecture during mouse postnatal development. *Invest Ophthalmol Vis Sci* 2010;51:2936-2942.

34. Buie LK, Karim MZ, Smith MH, Borras T. Development of a model of elevated intraocular pressure in rats by gene transfer of bone morphogenetic protein 2. *Invest Ophthalmol Vis Sci* 2013;54:5441-5455.

35. Elliott M, Gu X, Ashpole N, al e. Role of Caveolin-1 in conventional aqueous outflow pathway structure and function *ISER Sarasota Symposium, Sarasota, FL* 2013.

36. Kopczynski C, Novack GD, Swearingen D, van Haarlem T. Ocular hypotensive efficacy, safety and systemic absorption of AR-12286 ophthalmic solution in normal volunteers. *Br J Ophthalmol* 2013;97:567-572.

37. Crosson CE, Sloan CF, Yates PW. Modulation of conventional outflow facility by the adenosine A1 agonist N6-cyclohexyladenosine. *Invest Ophthalmol Vis Sci* 2005;46:3795-3799.

38. Heyne GW, Kiland JA, Kaufman PL, Gabelt BT. Effect of nitric oxide on anterior segment physiology in monkeys. *Invest Ophthalmol Vis Sci* 2013;54:5103-5110.

39. Stamer WD, Lei Y, Boussommier-Calleja A, Overby DR, Ethier CR. eNOS, a pressure-dependent regulator of intraocular pressure. *Invest Ophthalmol Vis Sci* 2011;52:9438-9444.

Figures

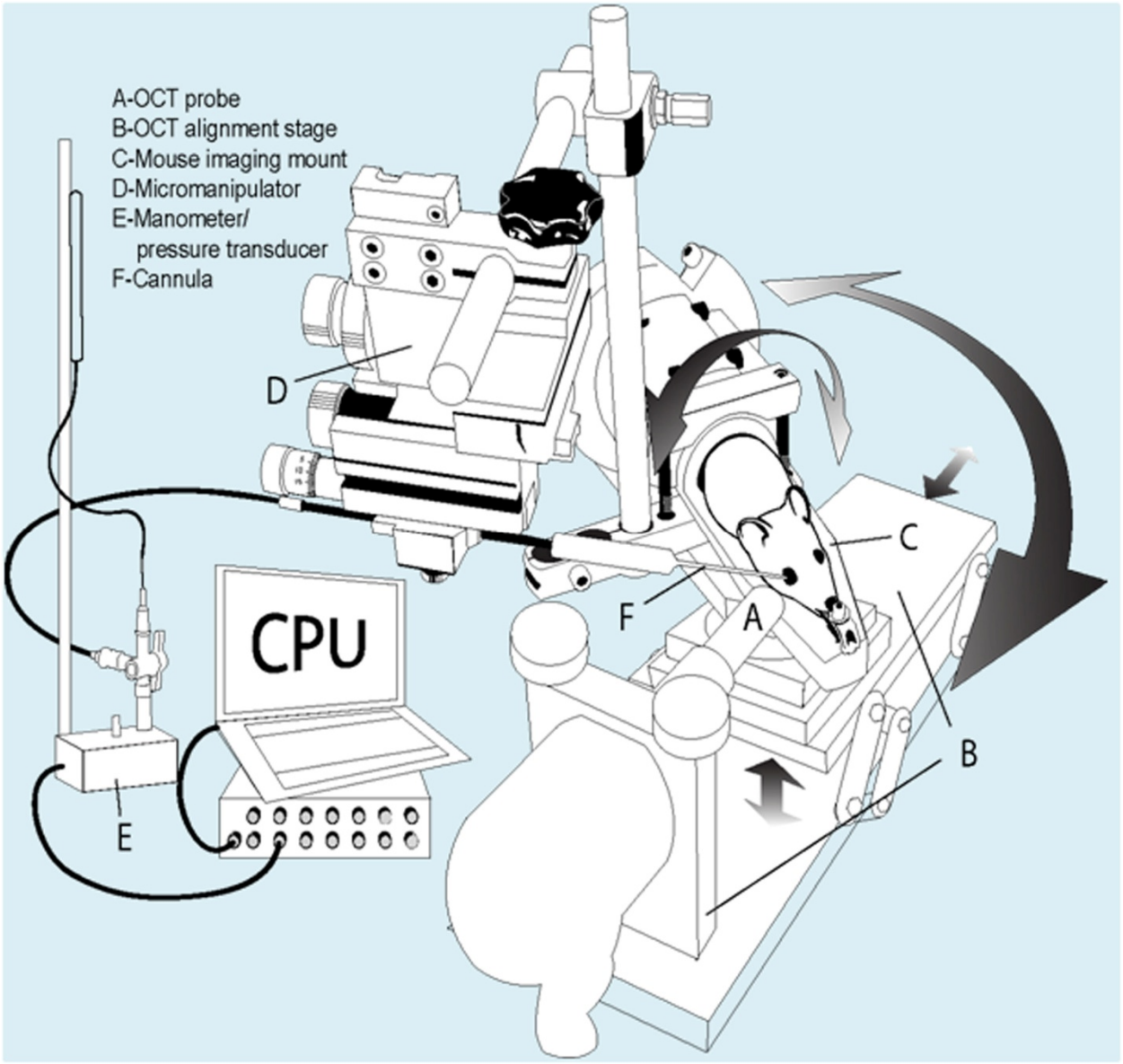

<u>Figure 1</u>. Schematic of custom-built experimental set-up for OCT imaging of mice. The system is designed intracameral drug delivery and control/monitoring of IOP while imaging. The custom mount (C) was machined to fit into a Bioptigen OCT alignment stage (B), enabling rotational and three dimensional positioning for precise focus of OCT probe (A) on iridio-corneo angle tissues. In addition, the mount was equipped with a micromanipulator (D) that rotates with mount for intracameral cannulations with glass micropipette (F). The glass microneedle cannula is connected to manometer and pressure transducer (E).

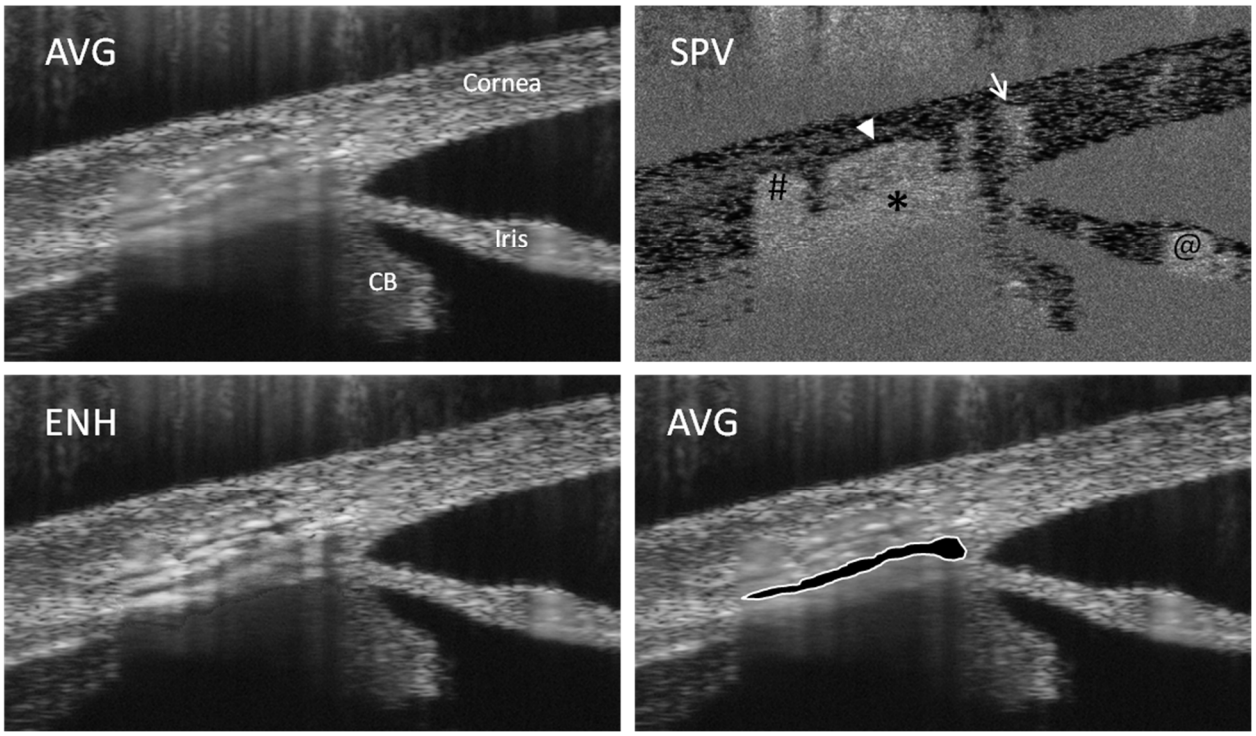

<u>Figure 2:</u> Comparison of three types of OCT images of the anterior angle of the mouse eye. Shown are two average intensity (AVG) images, a contrast enhanced (ENH) image and a speckle variance (SPV) image of the same region of a mouse anterior eye held at 10 mmHg. Arrow and hashmark show position of scleral vessels; arrowhead shows position of scleral vessel downstream of SC, asterisk shows the location of SC lumen, which is outlined and highlighted in lower right panel; CB=ciliary body; @=iris vessel.

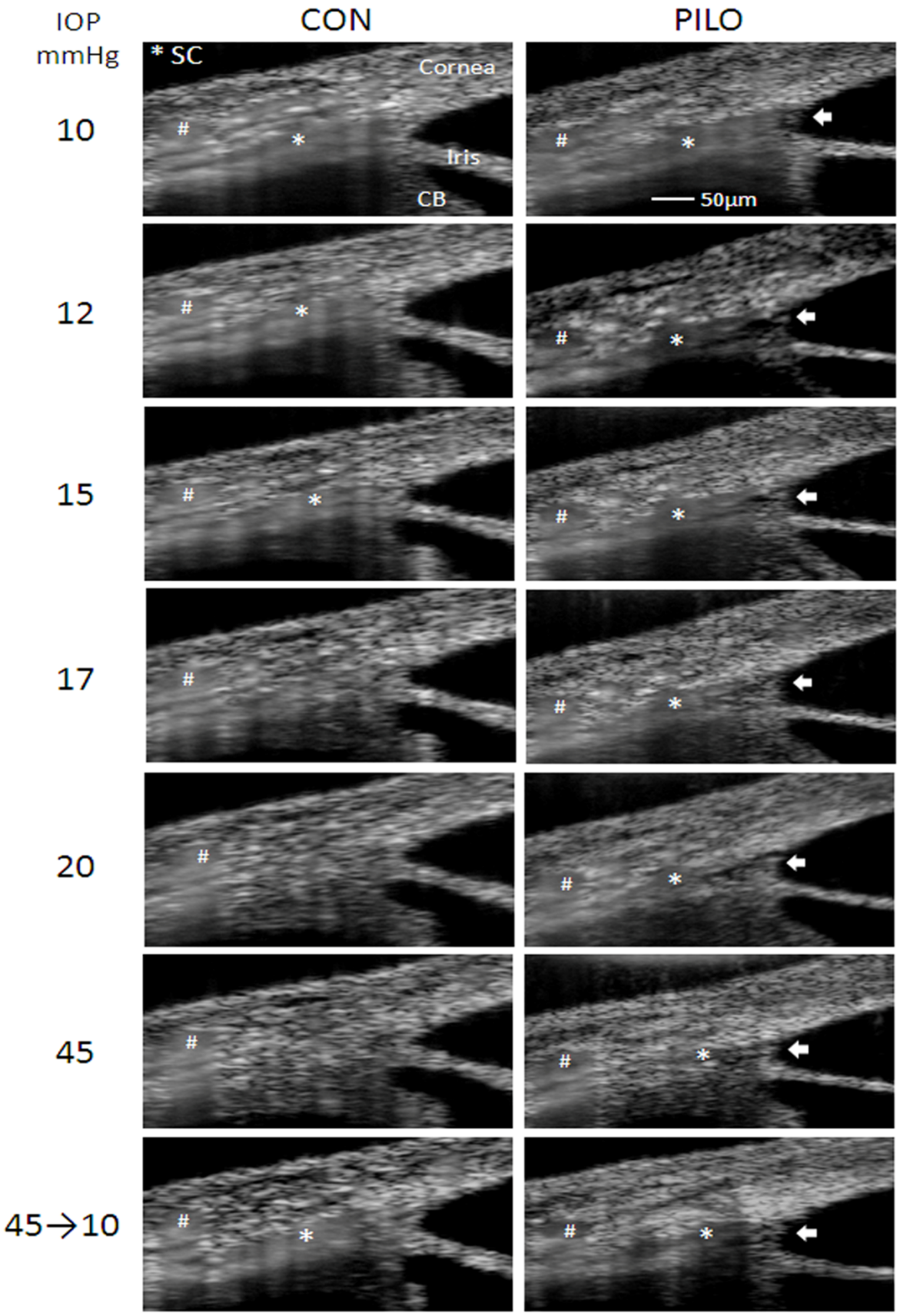
IOP
mmHg
CON
PILO
10
12
15
17
20
45
45→10
* SC
Cornea
Iris
CB
50μm
#
*

Figure 3. Examination of effects that sequential IOP steps have on SC lumen dimensions in mice, in the absence (CON) or presence of pilocarpine (PILO). Shown are averaged intensity SD-OCT images of iridio-corneo angle tissues containing SC lumen. Left column of images display effect of sequential IOP steps on SC lumen, marked by asterisk, from the same sagittal section. Note that due to image averaging, tissue with moving scatters (e.g. blood in vessels and SC) appear blurry. The effects of pilocarpine on SC lumen dimensions from the same sagittal section of the same mouse at sequential IOPs are shown in right column of images alongside untreated. Arrows indicate widening of the lamellated TM into an open fan-like shape, while hash marks show a scleral vessel that remains relatively unchanged during the imaging session. Shown are representative data from one mouse of 5 total mice that were examined. CB: ciliary body.

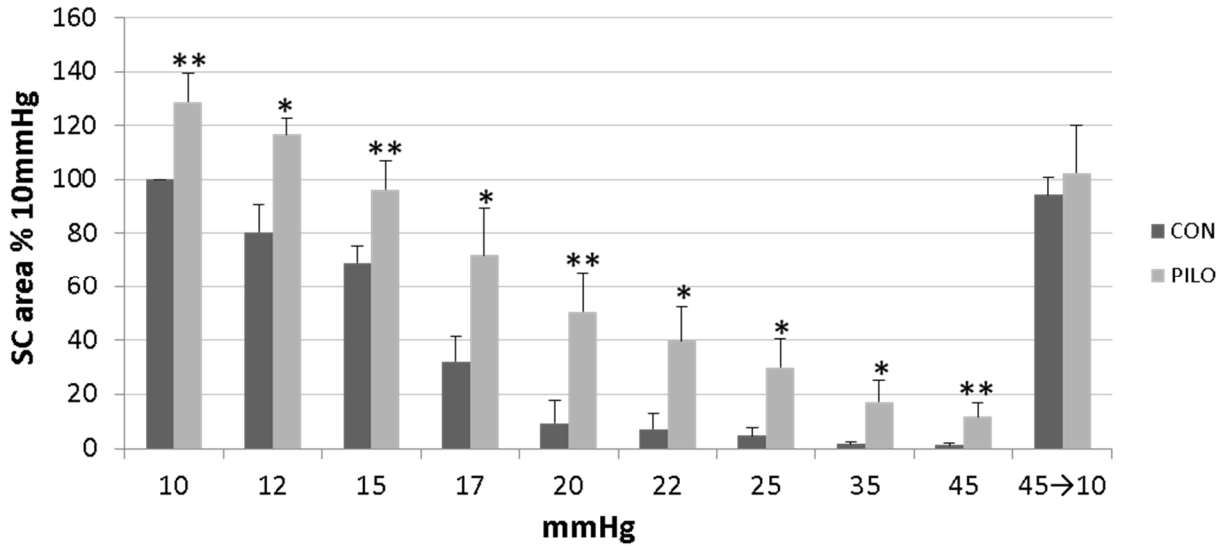

Figure 4. Quantitative analysis of SC lumen dimensions of mice exposed to different levels of IOP in the absence (CON) or presence of pilocarpine (PILO). Bar graph shows cumulative results obtained from OCT images of 4-5 total mice (mean ± SD), analyzing SC lumen area at each different condition. SC lumen area of each averaged OCT image was analyzed using ImageJ software on two separate occasions and two measurements were averaged for each condition. Data shown are normalized to initial SC area at 10 mmHg. Significant differences between untreated and pilocarpine-treated images are indicated (*$p<0.05$, **$p<0.01$)

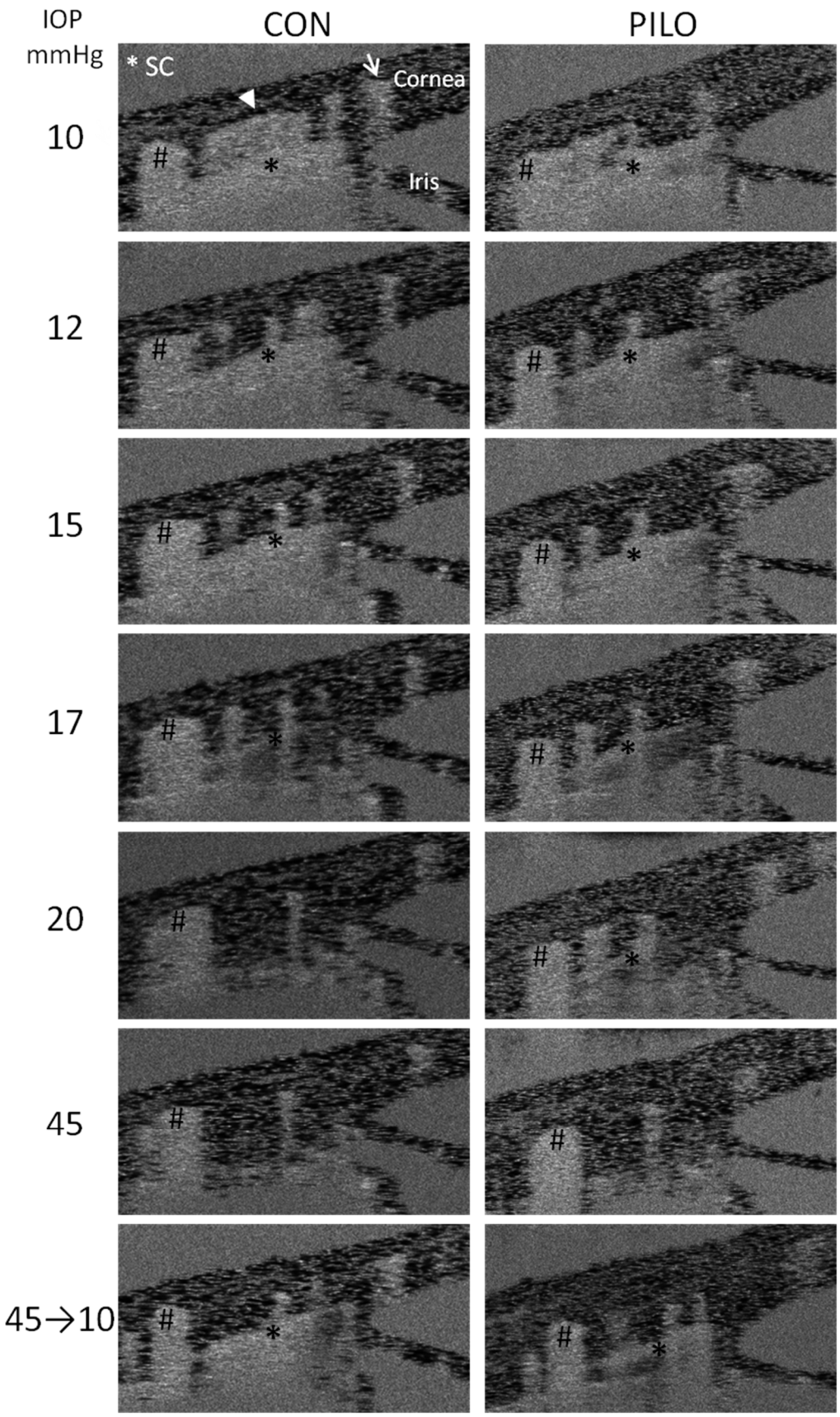
IOP
mmHg
CON
PILO
* SC
Cornea
Iris
10
12
15
17
20
45
45→10
#
*

Figure 5: Effects of sequential IOP steps on speckle variance in anterior eye of mouse in the absence (CON) or presence of pilocarpine (PILO). Shown are speckle variance OCT equivalents of the averaged images of iridio-corneo angle tissues containing SC lumen (*) in figure 3. Left column of images display effect of sequential IOP steps on speckle variance in SC lumen from the same sagittal section. Note that as IOP increases speckle variance in SC decreases, as well as does downstream scleral vessels (arrowhead) but not neighboring scleral vessels (# and arrow). The effects of pilocarpine on SC speckle variance from the same sagittal section of the same mouse at sequential IOPs are shown in right column of images alongside untreated. Shown are representative data from one mouse of 5 total mice that were examined.

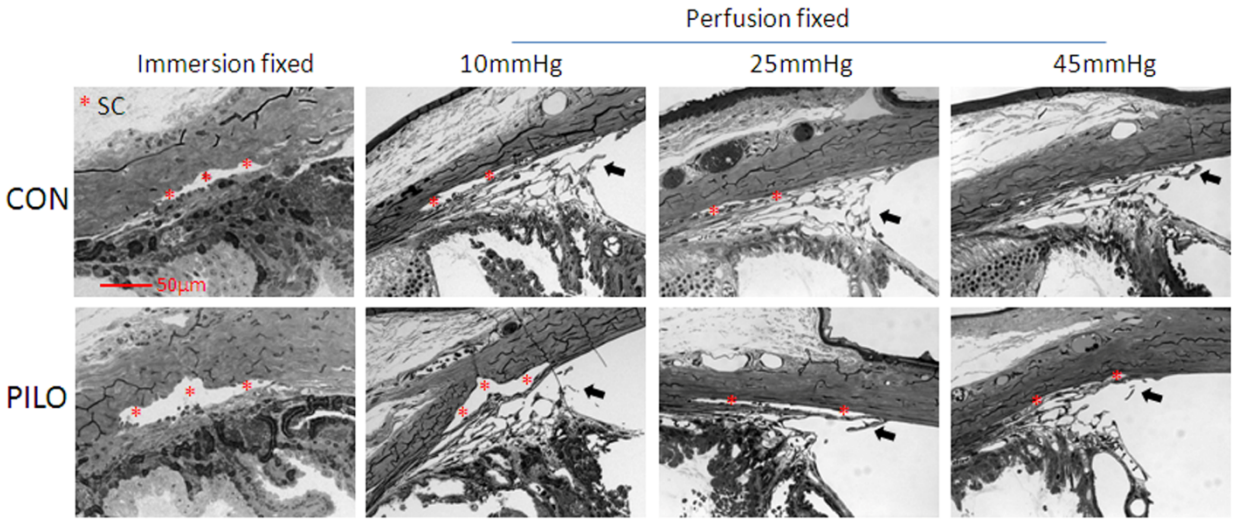

Figure 6. Standard histology of conventional outflow tissues in mouse eyes treated with pilocarpine. SC lumen of mouse eyes treated with pilocarpine (PILO) or PBS (CON) were examined. Eyes were treated and then fixed by immersion or perfusion at one of three intraocular pressures (10, 25 or 45 mmHg). Data show that SC lumen is more dilated regardless of fixation technique or perfusion pressure compared to control. Data are representative of images captured from 2 quadrants of 2 eyes for each condition. Arrows indicate pectinate ligaments with attached lamellated trabecular meshwork (TM) The widening of the TM and anterior chamber angle was not evaluated in these histological sections because of presumably artificial changes in the position of the iris and ciliary body during processing on account of the large lens.

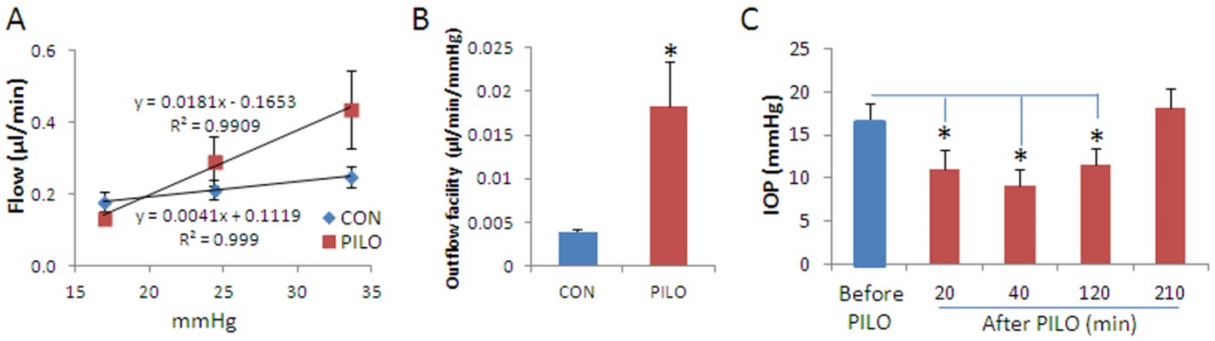

Figure 7. Outflow facility and intraocular pressure measurements in living mouse eyes treated with pilocarpine. Panel A shows pressure-flow relationship of paired iridotimized eyes, with one eye treated topically with PBS (CON) and the contralateral eye treated topically with 1% pilocarpine. Panel B shows the conventional outflow facility of pilocarpine-treated versus control eyes that was calculated as the slope of the flow versus pressure relationship shown in panel A. In a study of a separate cohort of anesthetized and iridotomized mice, panel C shows IOP that was measured using rebound tonometry (TonoLab) as a function of time after topical pilocarpine administration. Shown are mean data (± standard error of the mean) obtained from four mice (*$p<0.05$).

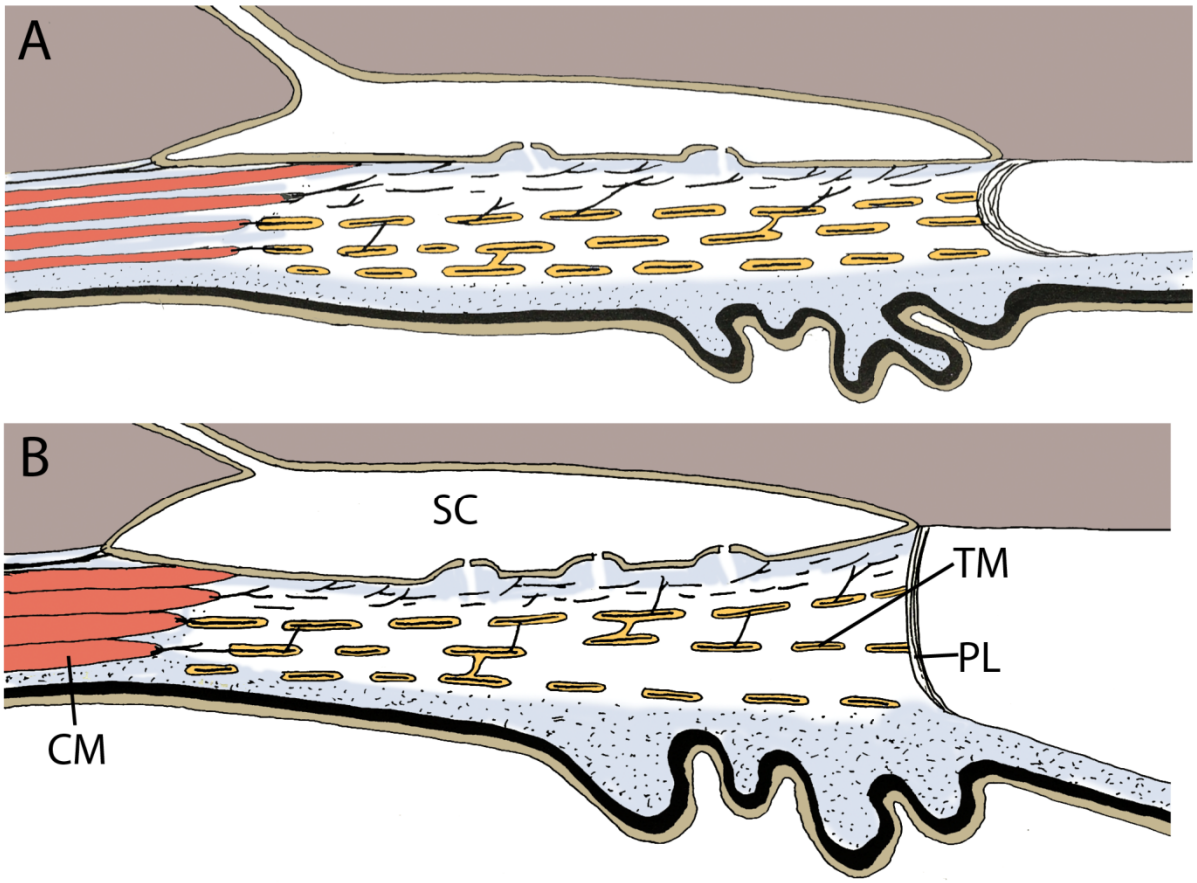

Figure 8: Schematic illustration of the effect of pilocarpine on the conventional outflow pathway in mouse eyes. Panel A: At physiological IOP without pilocarpine, the trabecular meshwork (TM) is collapsed with a small Schlemm's canal (SC). Panel B: Ciliary muscle (CM) contraction by pilocarpine widens the lumen of SC and expands the anterior lamellated TM into a fan-like shape, stretching the pectinate ligaments (PL).

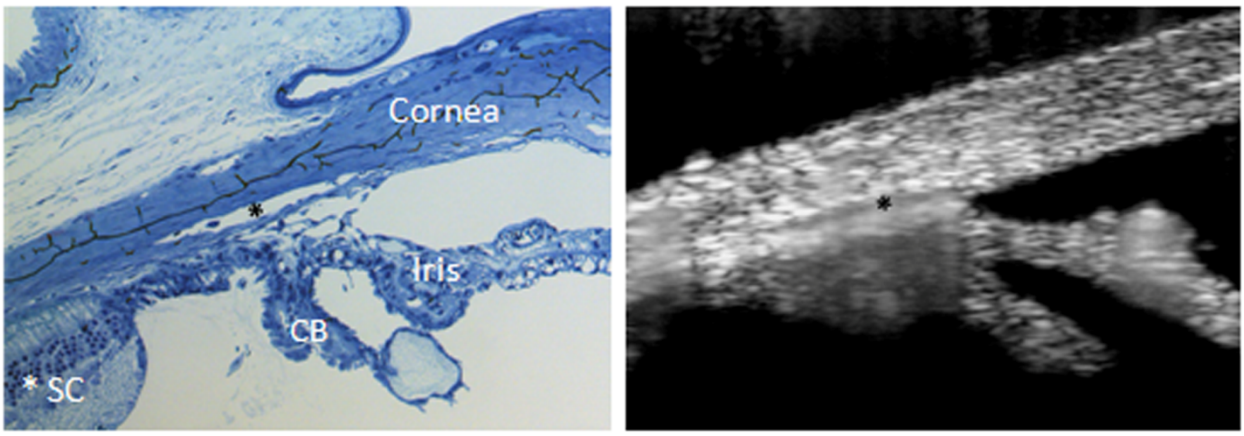

<u>Supplemental Figure 1</u>: **Comparison of Schlemm's canal lumen of mouse eyes by two methods.** Shown on left is a methylene blue-stained paraffin section of the anterior angle structures of an enucleated mouse eye visualized by light microscopy. On the right is an intensity averaged SD-OCT image of a living mouse eye at a similar anatomical location. Asterisks mark SC lumen; CB= ciliary body.

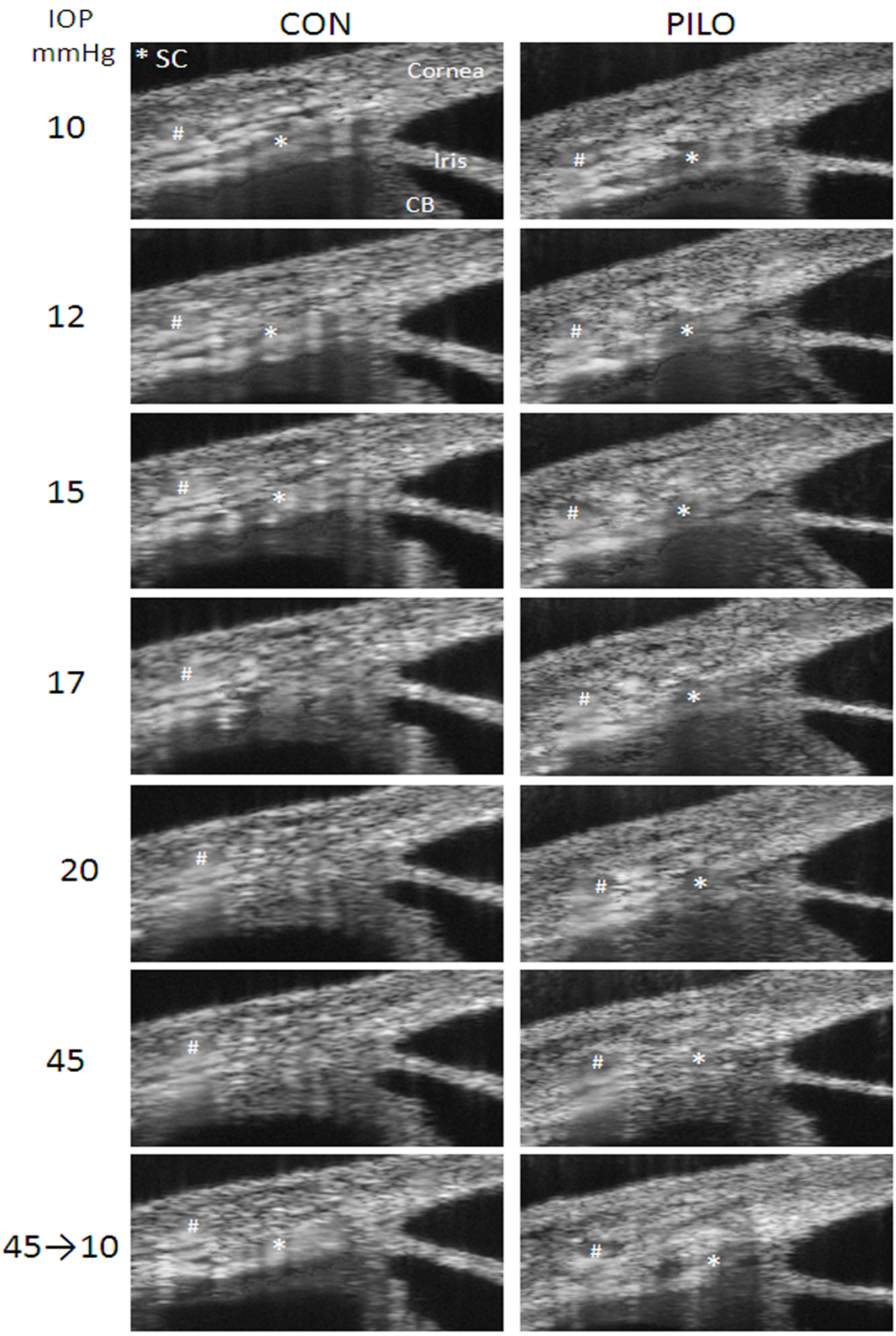
IOP
mmHg
CON
PILO
* SC
Cornea
Iris
CB
#
*
10
12
15
17
20
45
45→10

Supplemental Figure 2. Examination of effects that sequential IOP steps have on SC lumen dimensions in mice, in the absence (CON) or presence of pilocarpine (PILO). Shown are contrast enhanced SD-OCT images of iridio-corneo angle tissues containing SC lumen. Left column of images display effect of sequential IOP steps on SC lumen, marked by asterisk, from the same sagittal section. Note that due to image averaging, tissue with moving scatters (e.g. blood in vessels and SC) appear blurry. The hash mark indicates the location of a scleral vessel that does not change dimensions during imaging session. The effects of pilocarpine on SC lumen dimensions from the same sagittal section of the same mouse at sequential IOPs are shown in right column of images alongside untreated. Shown are representative data from one mouse of 5 total mice that were examined. CB: ciliary body.

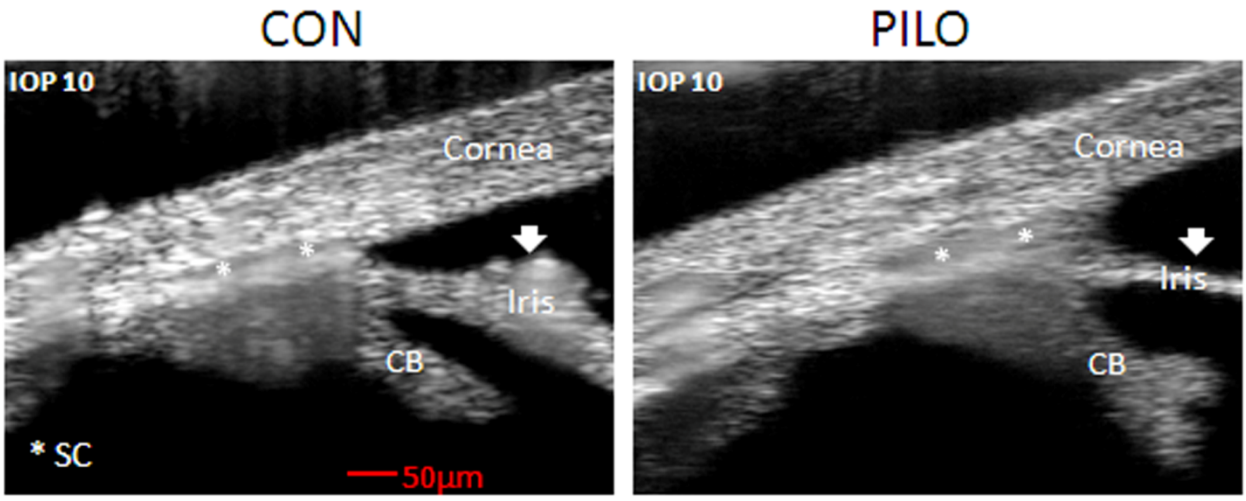

Supplemental Figure 3. Morphological changes of irideo-corneo angle tissues in mice induced by pilocarpine. Iridio-corneo angle tissues of anesthetized and iridotomized CD1 mice were imaged by SD-OCT (control, CON) and compared to images taken of same eye 10 minutes after application of one drop of 1% pilocarpine (PILO). The figures are representative of four individual experiments.

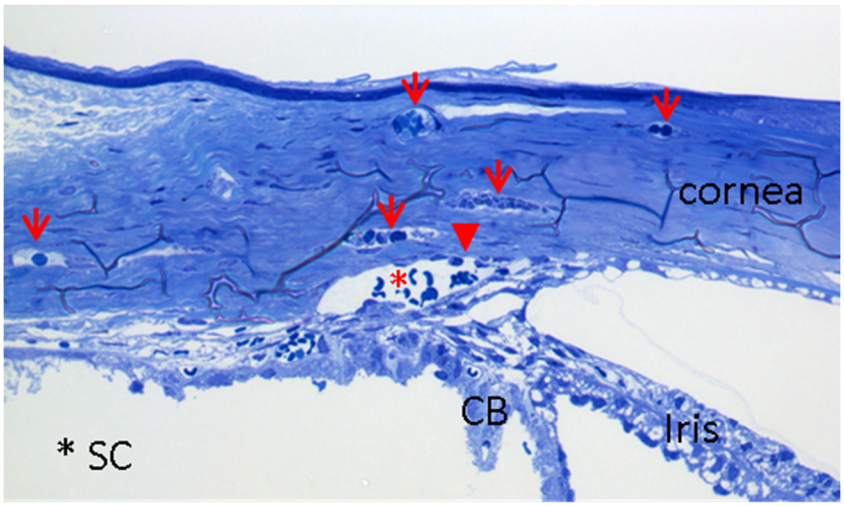

Figure 6. Standard histology of anterior angle tissues of mouse eye after OCT imaging session. Arrowhead points to red blood cells in Schlemm's canal (SC), while arrows mark red cells in scleral vessels. CB: ciliary body.